Journal Pre-proof

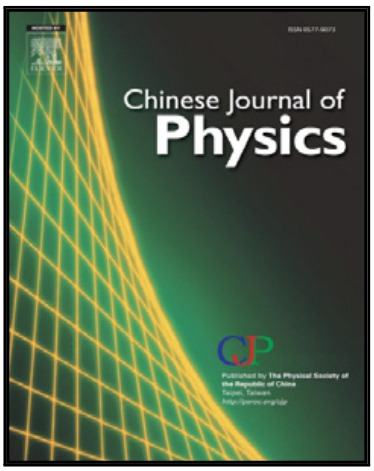

Toward non-degraded broadband room temperature terahertz detection by graphene plasmon-enhanced photo-thermoelectric effect

Songbin Meng , Lanxia Wang , Huiping Zhang , Anqi Yu , Xiaokai Pan , Qiwen Zhang , Xuguang Guo , Alexei V. Balakin , Alexander P. Shkurinov , YiMing Zhu

PII: S0577-9073(24)00142-4
DOI: https://doi.org/10.1016/j.cjph.2024.04.006
Reference: CJPH 2502

To appear in: *Chinese Journal of Physics*

Received date: 7 January 2024
Revised date: 31 March 2024
Accepted date: 6 April 2024

Please cite this article as: Songbin Meng , Lanxia Wang , Huiping Zhang , Anqi Yu , Xiaokai Pan , Qiwen Zhang , Xuguang Guo , Alexei V. Balakin , Alexander P. Shkurinov , YiMing Zhu , Toward non-degraded broadband room temperature terahertz detection by graphene plasmon-enhanced photo-thermoelectric effect, *Chinese Journal of Physics* (2024), doi: https://doi.org/10.1016/j.cjph.2024.04.006

Toward non-degraded broadband room temperature terahertz detection by graphene plasmon-enhanced photo-thermoelectric effect

Songbin Meng[1,†], Lanxia Wang[1,†], Huiping Zhang[1], Anqi Yu[1,*], Xiaokai Pan[2], Qiwen Zhang[3], Xuguang Guo[1,4], Alexei V. Balakin[1,5,6], Alexander P. Shkurinov[1,5,6], and YiMing Zhu[1,4,*]

[1] Shanghai Key Lab of Modern Optical System, Terahertz Technology Innovation Research Institute, Terahertz Spectrum and Imaging Technology Cooperative Innovation Center, University of Shanghai for Science and Technology, 516 Jungong Road, Shanghai 200093, China

[2] State Key Laboratory of Infrared Physics, Shanghai Institute of Technical Physics, Chinese Academy of Sciences, 500 Yutian Road, Shanghai 200080, China

[3] School of Optical-Electrical and Computer Engineering, University of Shanghai for Science and Technology, 516 Jungong Road, Shanghai 200093, China

[4] Shanghai Institute of Intelligent Science and Technology, Tongji University, 1239 Siping Road, Shanghai 200092, China

[5] Faculty of Physics and International laser Center, Lomonosov Moscow State University, Leninskie Gory 1-2, Moscow 19991 Russia

[6] ILIT RAS – Branch of the FSRC "Crystallography and Photonics" RAS, Svyatoozerskaya 1, 140700, Shatura, Moscow Region, Russia

[†] These authors contributed equally.

* Corresponding author. Tel: +86 021 5527-4272.

Highlights

- Terahertz detectors with asymmetric metal metamaterial show non-degraded response.
- Detectors with serial connection are inferred to show higher response.
- Detectors using graphene with higher mobility show higher response.
- Back gate tuning shows higher responsivity under negative back gate.

Graphical Abstract

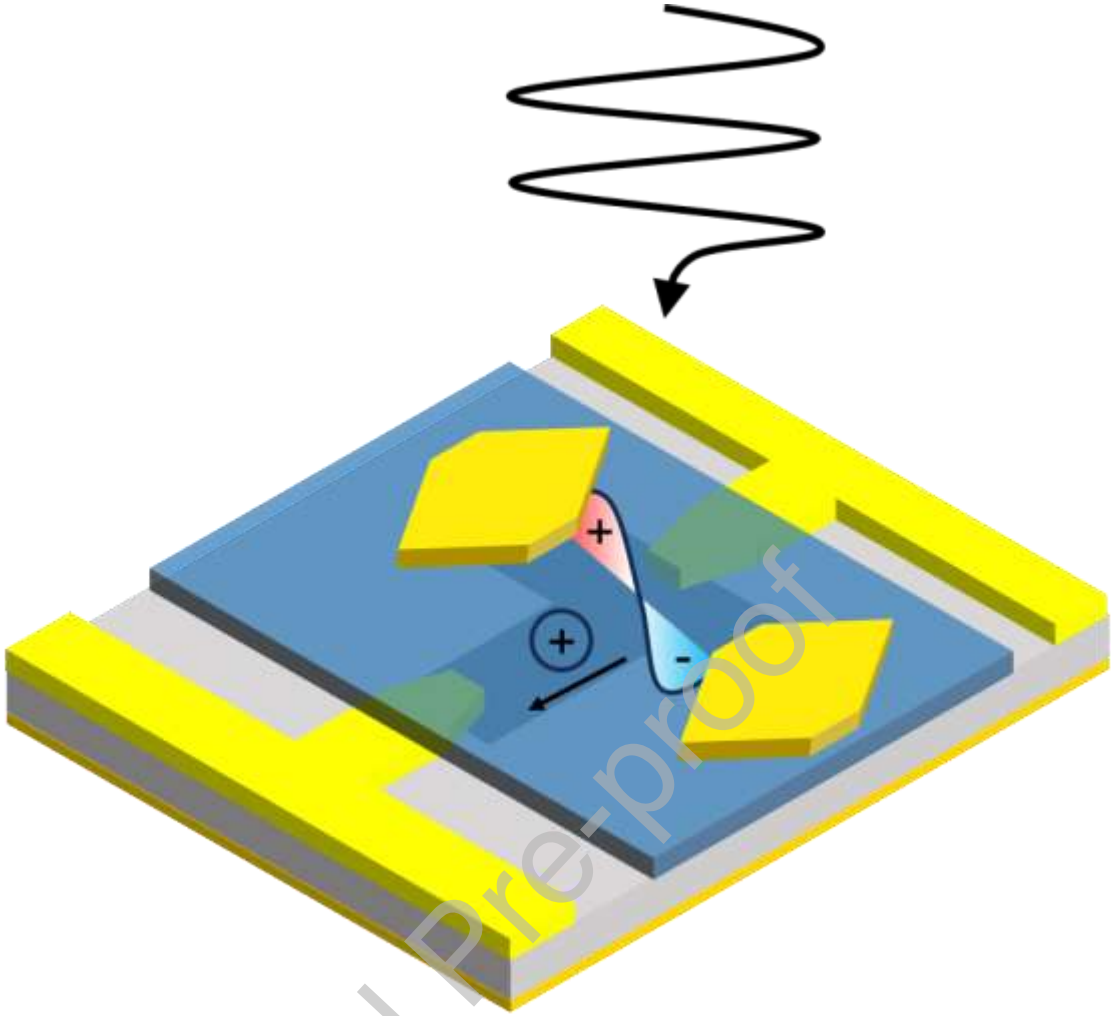

Abstract

In this work, we use T-shaped graphene as the channel of terahertz (THz) detector, and adopt metallic metamaterials near the source. Graphene plasmons at the source side are enhanced by the metallic metamaterials, increasing THz absorption and thus enhancing THz response generated by photo-thermoelectric effect. Because of the non-degraded absorption of graphene plasmons, samples with large metallic metamaterials show non-degraded response within 0.3 THz, and samples with small metallic metamaterials show non-degraded response within 0.75 THz. Series connection instead of parallel connection of each T-shaped graphene channel is expected to yield higher responsivity. Higher responsivity can also be achieved by applying back gate voltage. Samples using graphene with lower mobility show weaker response due to reduced THz absorption, and it is expected that higher response can be obtained by using graphene with higher mobility.

Introduction

The development of terahertz (THz) technology, which has great potential in safety [1,2], biomedicine [3,4], communication [5,6], and astronomy [7,8], has long lagged behind other frequencies. The low single photon energy limits the room temperature performance of photonic THz devices, and the high frequency limits the coupling efficiency between electronic THz

devices and incident waves. As a key component of THz technology, THz detector is still far from ideal, i.e., operating at room temperature with high responsivity, low noise equivalent power, broad bandwidth, short response time and large dynamic range. Up to now, commercial THz detectors mainly include pyroelectric detector, bolometer and Golay cells, in which pyroelectric detectors and Golay cells are slow, while bolometer usually need cryogenic environment. The breakthrough of terahertz detectors depends on: (i) new materials with special property, which can overcome the weakness of the prevailing detection mechanisms, (ii) new detection mechanism which has less weakness in terms of the above-mentioned characters, (iii) exquisite design which combines the properties of appropriate materials and mechanisms to realize all or most of the above-mentioned characters.

Since the discovery of graphene in 2004, two dimensional (2D) materials have been considered as promising material to ideal THz detector. In the past decade, many literatures reported THz detectors based on two dimensional materials, including bolometers [9-12], resonant [13,14] and non-resonant [15-21] plasma wave rectification detectors, photogalvanic detectors [22-25], and photo-thermoelectric (PTE) detectors [26-31]. Mittendorff et. al. demonstrated bolometer based on graphene with very short response time down to 50 ps, but the response was only 8 nA/W [9]. Detectors based on the resonant plasma wave rectification effect show a series of resonance peaks with high responsivity [13,14] and short response time [32]. Bandurin et. al. demonstrated resonant detection with responsivity up to 240 V/W at 10 K but much lower responsibity (< 10 V/W) at room temperature [13]. The major challenge for resonant plasma wave detection is fabrication of large-scale high-mobility material, since resonant detection requires $\omega\tau >> 1$ and typical commercial large-scale CVD-grown monolayer graphene shows $\tau < 50$ fs. Comparatively, non-resonant plasma wave rectification works efficiently within 1.5 THz. H. Qin et. al. demonstrated non-resonant plasma wave detection based on graphene with responsivity of 30 V/W and response time <5 μs [15]. The photogalvanic effect in type-II Dirac material was found efficient for terahertz detection in recent years. Guo et. al. fabricated $PdTe_2$ THz detector, the responsivity was 10 A/W with response time of 3.2 μs [22]. PTE detectors, which depend on the asymmetric diffusion of heated charge carriers, seems closest to ideal detectors. Castilla et. al. fabricated dipole antenna-coupled graphene-based PTE THz detector with detection range from 1.8-4.2 THz, peak responsivity of 105 V/W, response time < 30 ns, NEP of 80 $pW/Hz^{0.5}$, and dynamic range > 3 orders [26]. Viti et. al. reported PTE detector with response time down to 3.3 ns and peak responsivity of 49 V/W [27]. As it has been pointed out that the response time is proportional to channel length [29,30], further reducing response time need shorter channel length and using materials with short relaxation time of hot carriers. Because of the tradeoff between response time and responsivity, responsivity will be greatly reduced if response time is reduced to picosecond scale. Therefore, improvements must be done to raise responsivity. Two potential methods include contacting channel material with different materials to enhance the Seebeck coefficient or increasing THz absorption.

In this work, we adopted graphene as channel and excited graphene plasmons to enhance the THz absorption of graphene. Graphene plasmons are excited and enhanced by placing metallic metamaterial beside the source, but no metallic metamaterial is placed beside the drain, so that graphene plasmons will not be excited near the drain. Then charge carriers near the source will be heated much more than those near the drain, and the heated carriers diffuse from the source to the drain, generating PTE THz response. The broadband enhancement of metallic metamaterial on

graphene plasmons guarantees broadband absorption, and hence devices with large metallic metamaterials show non-degraded responsivity > 10 V/W within 0.3 THz, and devices with small metallic metamaterials show non-degraded responsivity > 1 V/W within 0.75 THz. Further enhancing responsivity can be realized by series connection of densely arranged detectors, tuning graphene Fermi level with a back gate, and using graphene with higher mobility. These results are helpful for designing broadband THz detector with high responsivity.

Experiment & Discussion

Fig. 1(a) schematically shows the structure of the samples. T-shaped graphene is used as channel, with horizontal bar defined as head (15 μm in x-coordinate and 5 μm in y-coordinate) and vertical ribbon defined as body (9 μm in x-coordinate and 15 μm in y-coordinate and). Golden truncated rhombus represents the metallic metamaterials, which is separated from graphene channel by a thin Al_2O_3 layer of 20nm. Detectors with different metamaterials are designed, including big rhombus (151 μm in x-coordinate and 145 μm in y-coordinate, used in Sample 1, Sample 5 and Sample 6), big triangle (truncated big rhombus without lower half triangle, used in Sample 2), small rhombus (21 μm in x-coordinate and 25 μm in y-coordinate, used in Sample 3), and small triangle (truncated big rhombus without lower half triangle, used in Sample 4). Source and Drain contacts of Samples 1-4 are 1 mm in width. Sample 1 and Sample 2 have 5 periodic T-shaped graphene, and Sample 3 and Sample 4 have 30 periodic T-shaped graphene, as schematically shown in Fig. 1(b-d). Sample 5 share the same design with Sample 1 in terms of metallic metamaterial, but have only one T-shaped graphene and a pair of big rhombuses.

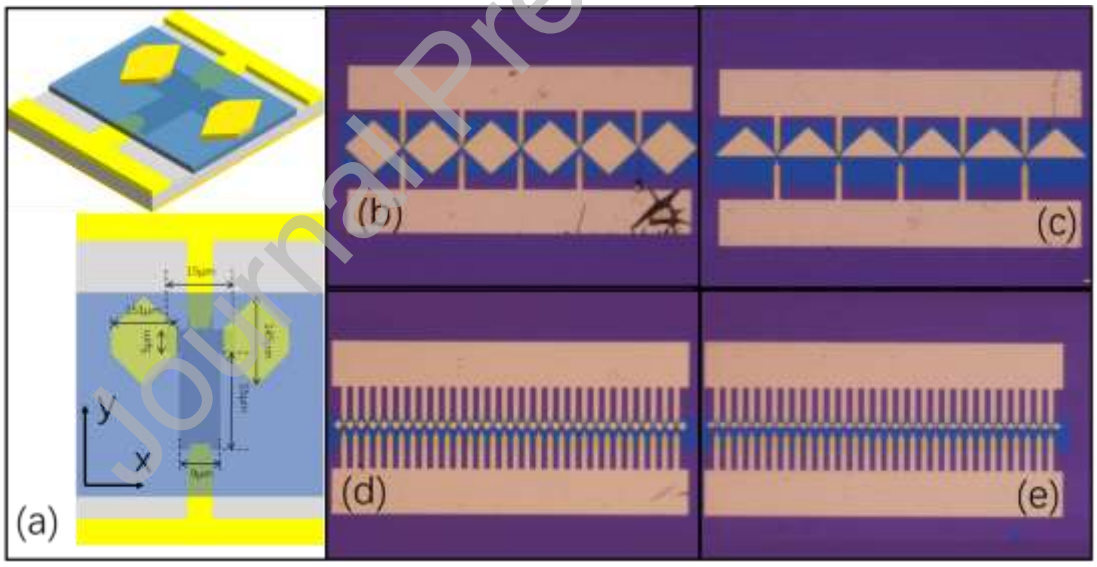

Fig. 1 (a) The schematics of the Sample 1. (b-f) The microscopic images of (b) Sample 1, (c) Sample 2, (d) Sample 3, (e) Sample 4.

In our previous work [33], graphene channel was 9 μm wide and 200 μm long, and showed resistance from 36000 Ω to 54000 Ω for a single graphene ribbon. In this work, the channel is 10 times shorter with the resistance of single T-shaped graphene varying from 3300 Ω to 5100 Ω, so the post-fabrication quality of graphene in this work is comparable with that in [33]. All four samples show response under 0 source-drain bias within 0.08 THz to 0.12 THz, where Sample 1 shows peak responsivity of 14.12 V/W, Sample 2 shows peak responsivity of 12.57 V/W, Sample

3 shows peak responsivity of 1.49 V/W and Sample 4 shows peak responsivity of 1.56 V/W, as shown in Fig. 2(b). Under 0.24 THz to 0.30 THz illumination, the peak responsivity of Sample 1 and Sample 2 slightly increases to 15.44 V/W and 16.69 V/W, respectively, and the peak responsivity of Sample 3 and Sample 4 keeps nearly unchanged (1.52 V/W and 1.59 V/W), as shown in Fig. 2(c). Under 0.24 THz to 0.3 THz illumination, Sample 1 and Sample 2 greatly reduces to 0.11 V/W and 0.089 V/W, but Sample 3 and Sample 4 show slightly higher response to 1.70 V/W and 1.92 V/W, as shown in Fig. 2(d).

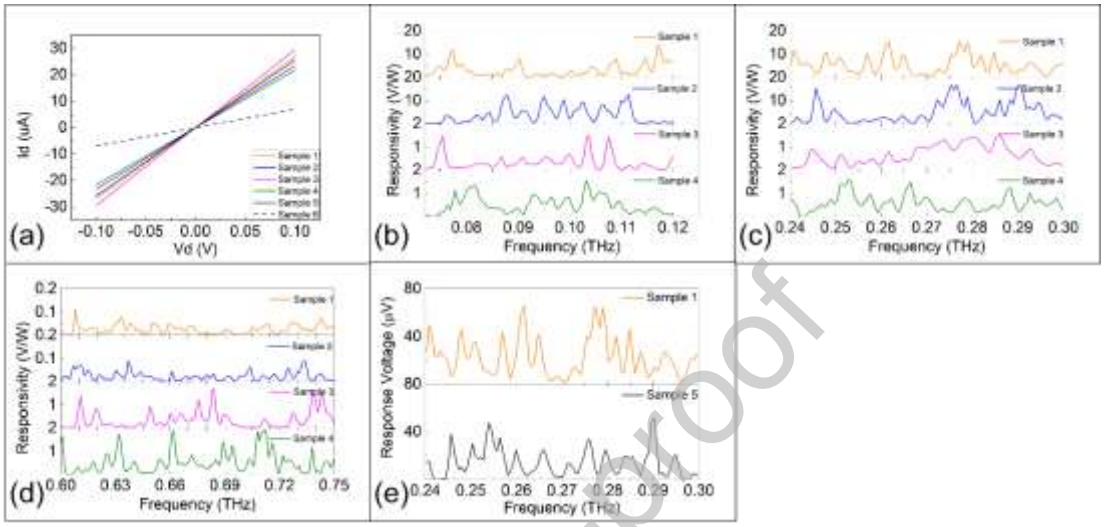

Fig. 2 (a) The measured IdVd curves normalized to a single T-shaped graphene of Samples 1-6. (b) The responsivity of Samples 1-4 from 0.08 THz to 0.12 THz. (c) The responsivity of Samples 1-4 from 0.24 THz to 0.30 THz. (d) The responsivity of Samples 1-4 from 0.60 THz to 0.75 THz. (e) The voltage response of Sample 1 and Sample 5 from 0.24 THz to 0.30 THz.

Here it should be noted that, an appealing merit of our samples, especially for Sample 3 and Sample 4, is non-degraded THz response, which is usually not observed in THz detectors using antennas, such as in [22,24]. FDTD simulation in Fig. 3(a) shows that the absorption of Sample 1and Sample 2 keeps non-degraded within 0.44 THz, and the absorption of Sample 3 and Sample 4 keeps non-degraded within 2.81 THz. Fig. 3(c) shows that the 1st order mode is about 0.44 THz for the metallic metamaterials used in Sample 1 and Sample 2, and about 2.81 THz for the metallic metamaterials used in Sample 3 and Sample 4. The correspondence between the 1st order mode and the cutoff frequency of high THz absorption suggests that the non-degraded THz absorption benefits from metallic metamaterials-enhanced graphene plasmons: metallic metamaterials functions as THz funnels, concentrating incident THz waves to the tips of metamaterials with high efficiency within first order mode of metamaterials. In this frequency range, the localized electric field around the tips of the metamaterials show slight increase as frequency increases, as shown in Fig. 3(d). Then graphene plasmons can be enhanced and show non-degraded absorption because of the enhanced localized electric field. When the incidence frequency is between the first order mode and the second order mode of the metallic metamaterials, the absorption of graphene plasmons decreases because of weakened electric field around the tips of metamaterials, as shown in Fig. 3(d). Such interaction between graphene plasmon modes and metamaterial resonance modes were discussed in detail in our previous work [34]. Then the non-degraded THz response is attributed to the non-degraded THz absorption.

Within 0.3 THz, Sample 1 and Sample 2 show higher THz absorption than Sample 3 and Sample 4, so that the THz response of Sample 1 and Sample 2 is stronger than Sample 3 and Sample 4. From 0.6 THz to 0.75 THz, the THz absorption of Sample 1 and Sample 2 greatly reduces and is even lower than that of Sample 3 and Sample 4, so that Sample 3 and Sample 4 show stronger response than Sample 1 and Sample 2.

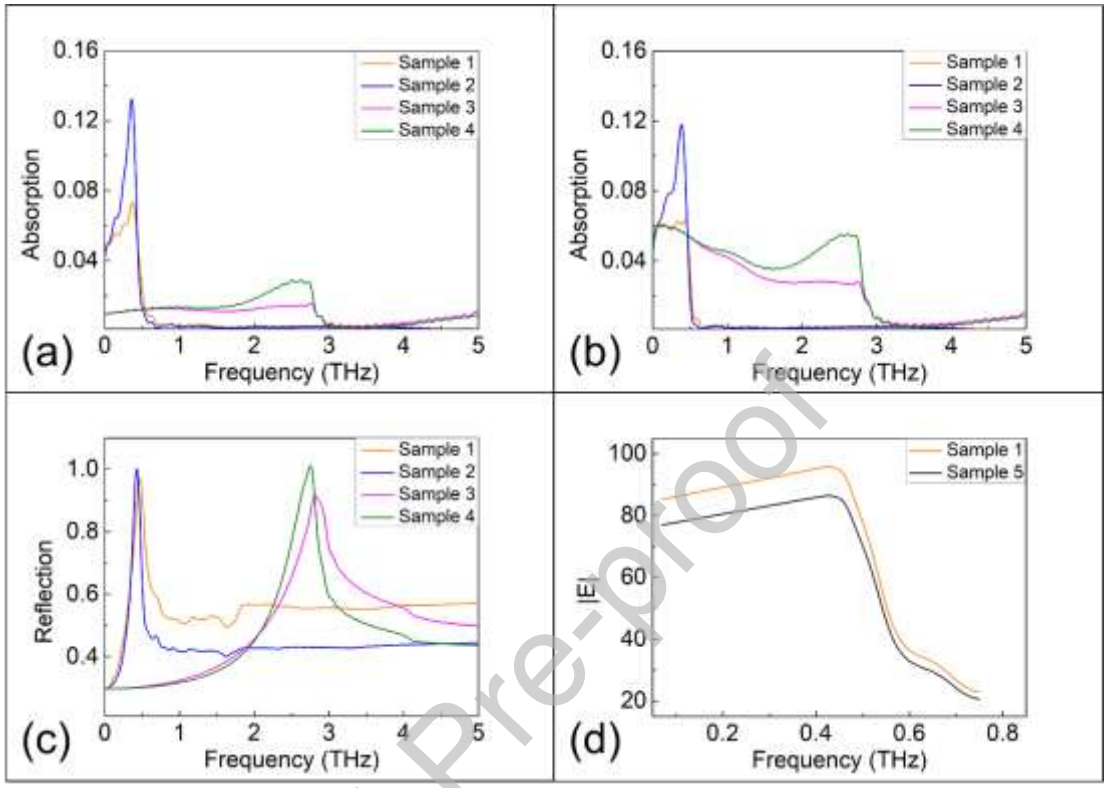

Fig. 3 (a) The absorption of Samples 1-4 by assuming the relaxing time of graphene to be 20 fs. (b) The absorption of Samples 1-4 by assuming the relaxing time of graphene to be 200 fs. (c) The reflection spectra of the metallic metamaterials used in Samples 1-4. (d) |E| under the tip of the metallic metamaterials from 0.05 THz to 1 THz when sparsely arranged (black curve) and densely arranged (orange curve).

In our previous work [33], metallic metamaterials were also used to enhance the excitation of graphene plasmons. However, because the structure was symmetric, plasmons excited near the source and near the drain have similar strength, and thus the response under 0 source-drain bias was very weak (measured peak current ~ 2 nA within 0.02 THz to 0.04 THz). In this work, metamaterials are placed only near the source, which promises strong asymmetry. Although the relaxation time τ of the charge carriers in graphene is possibly < 15 fs [33], which means that the excited plasmons near the source are overdamped, the enhanced THz absorption near the source will create temperature gradient from the source to the drain, generating stronger THz response than that reported in [33]. Besides, because response time of PTE detectors is proportional to channel length [29,30], the channel length is shortened from 200 μm [33] to 20 μm. Consequently, the response time reduces from 24 μs to 5 μs, as shown in Fig. 4(a).

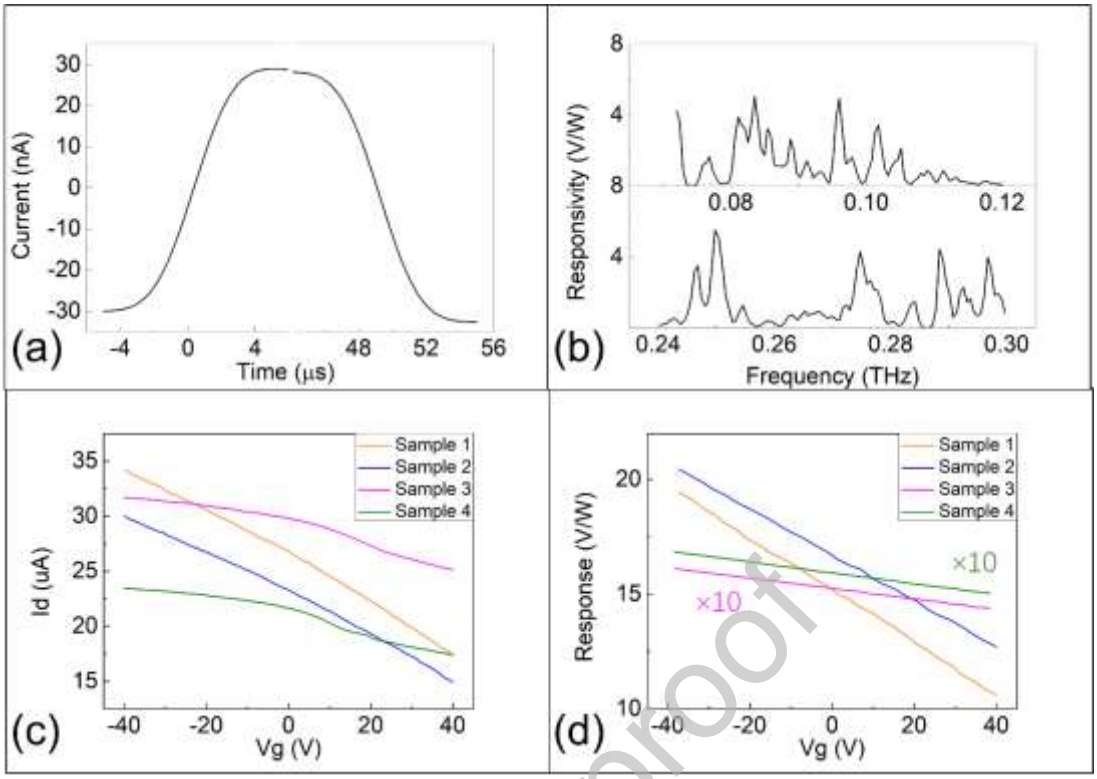

Fig. 4 (a) The measured response time of Sample 3. (b) THz responsivity of Sample 6 from 0.08 THz to 0.12 THz (upper panel) and from 0.24 THz to 0.30 THz (lower panel). (c) Transfer characteristic curves normalized to a single T-shaped graphene of Samples 1-4. (d) Response of the most significant peak as a function of back voltage within 0.24 THz to 0.3 TH of the Samples 1-4.

As the THz response of these samples depends on graphene plasmons-enhanced PTE effect, THz response can be further boosted in three aspects. The first one is adequate structure design. By comparing THz response of Sample 1 and Sample 5, one can see that their peak responses within 0.24 THz to 0.3 THz are similar, as shown in Fig. 2(e). In fact, Sample 1 can be considered as parallel connection of five single period, i.e., five Sample 5. As PTE detectors function as photo-induced voltage sources, parallel connection will not induce in larger output voltage. Compared with parallel connection, series connection will generate higher voltage response, if the localized electric field around the tips of the densely arranged metamaterials share similar strength with that around the tips of sparsely arranged metamaterials. To answer this question, we simulated sparsely arranged big rhombus (like in Sample 5) and densely arranged big rhombus (like in Sample 1). Fig. 3(d) shows that the average |E| under the tips of densely arranged big rhombus is slightly higher than that in sparsely arranged big rhombus. Then it is reasonable that the plasmons excited in Sample 1 share similar strength with those excited in Sample 5, which is possibly the reason for the similar peak response. Based on this simulation result, it can be anticipated that Sample 1 could have generated 4 times higher response if it were designed as a series connection of Sample 5 instead of a parallel one. Similarly, Sample 3 and Sample 4 could have generated 29 times higher response in the same way. In that case, Sample 3 and Sample 4 may generated higher response than Sample 1 and Sample 2. The reason is that a single period of Sample 1 (/Sample 2) is more than 25 times larger than that of Sample 3 (/Sample 4), while the

responsivity of Sample 1 (/Sample 2) is just 10 times larger than that of Sample 3 (/Sample 4). If all these samples are replaced by series connection, i.e., forming a PTE pile, with similar area, Sample 3 and Sample 4 will possibly generate twice stronger responsivity. Considering that a single period of Sample 4 is even smaller than a single period of Sample 3 and they show similar THz response from 0.072 THz to 0.75 THz (and Sample 4 is expected to show higher response from 2 THz to 3 THz according to the simulation shown in Fig. 3(a)), a series connection of single period of Sample 4 will generate largest THz response because of the largest amount of single period. Therefore, design of detectors with small metallic metamaterial in series connection is possibly helpful in boosting the THz responsivity. Alternatively, a combination of the proposed structure and broadband metalens [35,36] can also help to boost the THz responsivity by raising the localized electric field.

The second aspect lies in increasing the THz absorption of graphene plasmons by using graphene with higher mobility. By comparing Fig. 3(a) and Fig. 3(b), one can see that the THz absorption of graphene plasmons decreases from > 4% to ~ 1% within 1.0 THz, when the relaxation time reduces from 200 fs to 20 fs. In the experiment, we fabricated Sample 6, which share the same structure with Sample 1, but using graphene with pre-fabrication mobility of 1000 cm^2/Vs. As shown in Fig 1(a), the measured current of Sample 6 is about 3-4 times lower than that of Samples 1-5, corresponding to their difference in mobility. Fig 4(b) shows that the responsivity of Sample 6 is lower than half that of Sample 1. We attribute the weakening in responsivity to the reduction in absorption. This indicates that higher responsivity can be expected for detectors by using graphene with mobility > 10^4 cm^2/Vs.

The last aspect lies in enhancing the Seebeck coefficient of graphene. Generally, PTE THz detectors show peak responsivity at certain gate voltage [16]. However, all samples in this work show limited back gate tunability because of the poor conductivity of Si substrate. The measured current only changes by 96.6%, 100.6%, 26.1% and 34.3% for Sample 1, Sample 2, Sample 3 and Sample 4, respectively, as the back gate voltage increases from -40 V to 40 V. The decrease in current as back gate voltage increases as shown in Fig. 4(c) indicates hole domination. Correspondingly, the responsivity only increases by 26.3%, 21.2%, 5.8% and 5.9% for Sample 1, Sample 2, Sample 3 and Sample 4, respectively, as the back gate voltage reduces from 0 V to -40 V (Fig. 4(d)). According to our previous work [33], larger increase in responsivity is expected if mediumly-doped Si substrate is used.

Conclusions

To conclude, we fabricated THz detectors using T-shaped graphene and metallic metamaterials. Benefiting from metallic metamaterials-enhanced broadband THz absorption of graphene plasmons, these detectors show non-degraded plasmon-assisted PTE THz response within low-THz region. Higher zero bias responsivity and shorter response time are achieved by asymmetric design of metallic metamaterial and shortening graphene channel. Detectors with large metallic metamaterials show higher responsivity, and detectors with small metallic metamaterials show broader frequency range with non-degraded responsivity. Detectors with small metallic metamaterials are expected to show higher responsivity by series connection of dense arrangement with similar area. Further enhancement in responsivity includes using graphene with higher mobility, and enhancing Seebeck coefficient of graphene by efficient gate tuning.

EXPERIMENTAL SECTION

Device Fabrication. Commercial CVD-grown monolayer graphene with pre-fabrication mobility of 3000 cm^2/Vs, the same as that used in our previous work [33], is used as channel for Samples 1-5, and CVD-grown graphene with pre-fabrication mobility of 1000 cm^2/Vs, is used as channel for Sample 6. Graphene is wet-transferred onto Si/SiO_2 substrate, with Si thickness of 500 μm and resistivity $>10^3$ Ω·cm, and SiO_2 thickness of 300 nm. After that, the graphene flake is patterned into periodic T-shape by O_2 ion. Two large metal pads (Cr/Au 20/80 nm) functions as source and drain, with the source connecting the head of T-shaped graphene and the drain connecting the end of body. Metallic metamaterials (Au 80 nm) are placed between the heads of T-shaped graphene, with overlap region of 3 μm. The thin Al_2O_3 layer, which separate T-shaped graphene and metallic metamaterial, is used to guarantee enhanced localized electric field between metallic metamaterial and graphene.

Measurements. All the measurements were performed at room temperature and under ambient environment. IdVd, IdVg curves are measured by using a Source/Measurement Unit (Agilent B2912A). We used a microwave source (Agilent E8257D, 20-40 GHz) equipped with VDI multipliers (WR 2.8 and WR 9 Tripler) to generate THz signal from 0.072 THz to 0.12 THz, and from 0.24 THz to 0.30 THz. A microwave source (Agilent E8257D, 9-13 GHz) with a 54x frequency multiplier is used to generate THz signal from 0.60 THz to 0.75 THz. THz response was measured by combining the Source/Measurement Unit with a lock-in amplifier (SR830) and a high-speed sampling oscilloscope. Responsivity was calculated by $R=I/P*S_{eff}$, where I is the measured response current, P is the power density of THz signal, and is 1 mW/cm^2 for 0.072-0.12 THz and 0.24-0.30 THz, and 0.2 mW/cm^2 for 0.60-0.75 THz, S_{eff} is the effective detector area calculated by $S_{eff} = \max\{S_{dev}, S_{THz}\}$, where $S_{dev} = 0.424\ mm^2$ is the detector area, and $S_{THz} = \lambda^2/4\pi$ is the diffraction-limited area.

Acknowledgments

This work was supported in part by the National Natural Science Foundation of China (62201349), in part by the 111 Project (D18014), in part by the General Administration of Customs People's Republic of China (2019HK006), in part by the State assignment FSRC «Crystallography and Photonics» RAS.

References

[1] Y. C. Shen, T. Lo, P. F. Taday, B. E. Cole, W. R. Tribe and M. C. Kemp, "Detection and identification of explosives using terahertz pulsed spectroscopic imaging", Appl Phys. Lett. 86, 241116 (2005).

[2] H.-B. Liu, Y. Chen, G. J. Bastiaans and X.-C. Zhang, "Detection and identification of explosive RDX by THz diffuse reflection spectroscopy", Opt. Express14, 415-423 (2006).

[3] S. M. Kim, F. Hatami and J. S. Harris, "Biomedical terahertz imaging with a quantum cascade laser", Appl. Phys. Lett. 88, 153903 (2006).

[4] Y. Peng, J. Huang, J. Luo, Z. Yang, L. Wang, X. Wu, X. Zang, C. Yu, M. Gu, Q. Hu, X. Zhang, Y. Zhu, and S. Zhuang, "Three-step one-way model in terahertz biomedical detection", Photonix, 2, 12 (2021).

[5] M. Kim, E. Pallecchi, R. Ge, X. Wu, G. Ducournau, J. C. Lee, H. Happy, and D. Akinwande, "Analogue switches made from boron nitride monolayers for application in 5G and terahertz

communication systems", Nat. Electron. 3, 479-485 (2020).

[6] T. Harter, C. Füllner, J. N. Kemal, S. Ummethala, J. L. Steinmann, M. Brosi, J. L. Hesler, E. Bründermann, A.-S. Müller, W. Freude, S. Randel, and C. Koos, "Generalized Kramers-Kronig receiver for coherent terahertz communications", Nat. Photonics 14, 601-606 (2020).

[7] C. Kulesa, "Terahertz spectroscopy for astronomy: from comets to cosmology", IEEE Trans. Terahertz Sci. Technol. 1, 232-240(2011).

[8] S. Ishii, M. Seta, N. Nakai, S. Nagai, N. Miyagawa, A. Yamauchi, H. Motoyama, and M. Taguchi, "Site testing at Dome Fuji for submillimeter and terahertz astronomy: 220 GHz at atmospheric-transparency", Polar Sci. 3, 213-221 (2010).

[9] M. Mittendorff, S. Winnerl, J. Kamann, J. Eroms, D. Weiss, H. Schneider, and M. Helm, "Ultrafast graphene-based broadband THz detector", Appl. Phys. Lett. 103, 021113 (2013).

[10] A. El Fatimy, R. L. Myers-Ward, R., Boyd, A. K. Boyd, K. M. Daniels, D. K. Gaskill, and P. Barbara, "Epitaxial graphene quantum dots for high-performance terahertz bolometers", Nat. Nanotechnol. 11, 335–338 (2016).

[11] W. Miao, H. Gao, Z. Wang, W. Zhang, Y. Ren, K. M. Zhou, S. C. Shi, C. Yu, Z. Z. He, Q. B. Lin, and Z. H. Feng, "A graphene-based terahertz hot electron bolometer with Johnson noise readout", J. Low Temp. Phys. 193, 387–392 (2018).

[12] L. Viti, J. Hu, D. Coquillat, A. Politano, W. Knap, and M. S. Vitiello, "Efficient Terahertz detection in black-phosphorus nano-transistors with selective and controllable plasma-wave, bolometric and thermoelectric response". Sci. Rep. 6, 20474 (2016).

[13] D. A. Bandurin, D. Svintsov, I. Gayduchenko, S. G. Xu, A. Principi, M. Moskotin, I. Tretyakov, D. Yagodkin, S. Zhukov, T. Taniguchi, K. Watanabe, I. V. Grigorieva, M. Polini, G. N. Goltsman, A. K. Geim, and G. Fedorov, "Resonant terahertz detection using graphene plasmons", Nat. Commun. 9, 5392 (2018).

[14] V. Ryzhii, N. Ryabova, M. Ryzhii, N. V. Baryshnikov, V.E. Karasik, V. Mitin, and T. Otsuji, "Terahertz and infrared photodetectors based on multiple graphene layer and nanoribbon structures", Opto-Electron. Rev. 20, 15-25 (2012).

[15] H. Qin, J. Sun, S. Liang, X. Li, X. Yang, Z. He, C. Yu, and Z. Feng, "Room-temperature, low-impedance and high-sensitivity terahertz direct detector based on bilayer graphene field-effect transistor", Carbon 116, 760-765 (2017).

[16] D. A. Bandurin, I. Gayduchenko, Y. Cao, M. Moskotin, A. Principi, I. V. Grigorieva, G. Goltsman, G. Fedorov, and D. Svintsov, "Dual origin of room temperature sub-terahertz photoresponse in graphene field effect transistors", Appl. Phys. Lett. 112, 141101 (2018).

[17] L. Viti, J. Hu, D. Coquillat, W. Knap, A. Tredicucci, A. Politano, and M. S. Vitiello, "Black Phosphorus terahertz photodetectors", Adv. Mater. 27, 5567-5572 (2015).

[18] F. Bianco, D. Perenzoni, D. Convertino, S. L. De Bonis, D. Spirito, M. Perenzoni, C. Coletti, M. S. Vitiello, and A. Tredicucci, "Terahertz detection by epitaxial-graphene field-effect-transistors on silicon carbide", Appl. Phys. Lett. 107, 131104(2015).

[19] D. Spirito, D. Coquillat, S. L. De Bonis, A. Lombardo, M. Bruna, A. C. Ferrari, V. Pellegrini, A. Tredicucci, W. Knap, and M. S. Vitiello, "High performance bilayer-graphene terahertz detectors", Appl. Phys. Lett. 104, 061111(2014).

[20] A. Zak, M. A. Andersson, M. Bauer, J. Matukas, A. Lisauskas, H. G. Roskos, and J. Stake, "Antenna-integrated 0.6 THz FET direct detectors based on CVD graphene", Nano Letters. 14, 5834-5838(2014).

[21] L. Vicarelli, M. S. Vitiello, D. Coquillat, A. Lombardo, A. C. Ferrari, W. Knap, M. Polini, V. Pellegrini, and A. Tredicucci, "Graphene field-effect transistors as room-temperature terahertz detectors", Nat. Mater. 11, 865–871 (2012).

[22] C. Guo, Y. Hu, G. Chen, D. Wei, L. Zhang, Z. Chen, W. Guo, H. Xu, C.-N. Kuo, C. S. Lue, X. Bo, X. Wan, L. Wang, A. Politano, X. Chen, and W. Lu, "Anisotropic ultrasensitive $PdTe_2$-based phototransistor for room-temperature long-wavelength detection", Sci. Adv. 6, eabb6500 (2020).

[23] L. Zhang, C. Guo, C.-N. Kuo, H. Xu, K. Zhang, B. Ghosh, J. De Santis, D. W. Boukhvalov, I. Vobornik, V. Paolucci, C. S. Lue, H. Xing, A. Agarwal, L. Wang, and A. Politano, "Terahertz photodetection with type-II Dirac fermions in transition-metal ditellurides and their heterostructures", Phys. Status Solidi RRL 2100212 (2021).

[24] Y. Yang, K. Zhang, L. Zhang, G. Hong, C. Chen, H. Jing, J. Lu, P. Wang, X. Chen, L. Wang, and H. Xu, "Controllable growth of type-II Dirac semimetal $PtTe_2$ atomic layer on Au substrate for sensitive room temperature terahertz photodetection", InfoMat. 3, 705-715 (2021).

[25] H. Xu, F. Fei, Z. Chen, X. Bo, Z. Sun, X. Wan, L. Han, L. Wang, K. Zhang, J. Zhang, G. Chen, C. Liu, W. Guo, L. Yang, D. Wei, F. Song, X. Chen, and W. Lu, "Colossal terahertz photoresponse at room temperature: a signature of type-II Dirac Fermiology", ACS Nano 15, 5138-5146 (2021).

[26] S. Castilla, B. Terrés, M. Autore, L. Viti, J. Li, A. Y. Nikitin, I. Vangelidis, K. Watanabe, T. Taniguchi, E. Lidorikis, M. S. Vitiello, R. Hillenbrand, K.-J. Tielrooij, and F. H. L. Koppens, "Fast and sensitive terahertz detection using an antenna-integrated graphene pn junction", Nano Lett. 19, 2765-2773 (2019).

[27] L. Viti, D. G. Purdie, A. Lombardo, A. C. Ferrari, and M. S. Vitiello, "HBN-encapsulated, graphene-based, room-temperature terahertz receivers, with high speed and low noise", Nano Lett. 20, 3169-3177 (2020).

[28] M. Asgari, E. Riccardi, O. Balci, D. De Fazio, S. M. Shinde, J. Zhang, S. Mignuzzi, F. H. L. Koppens, A. C. Ferrari, L. Viti, and M. S. Vitiello, "Chip-scalable, room-temperature, zero-bias, graphene-based terahertz detectors with nanosecond response time", ACS Nano 15, 17966-17976 (2021).

[29] W. Guo, Z. Dong, Y. Xu, C. Liu, D. Wei, L. Zhang, X. Shi, C. Guo, H. Xu, G. Chen, L. Wang, K. Zhang, X. Chen, and W. Lu, "Sensitive terahertz detection and imaging driven by the photothermoelectric effect in ultrashort-channel black phosphorus devices", Adv. Sci. 1902699 (2020).

[30] X. Deng, Y. Wang, Z. Zhao, Z. Chen, and J. Sun, "Terahertz-induced photothermoelectric response in graphene-metal contact structures", J. Phys. D: Appl. Phys. 49, 425101 (2016).

[31] X. Cai, A. B. Sushkov, R. J. Suess, M. M. Jadidi, G. S. Jenkins, L. O. Nyakiti, R. L. M.-Ward, S. Li, J. Yan, D. K. Gaskill, T. E. Murphy, H. D. Drew, and M. S. Fuhrer, "Sensitive room-temperature terahertz detection via the photothermoelectric effect in graphene", Nat. Nanotechnol. **9**, 814-819 (2014).

[32] S. Kim, J. D. Zimmerman, P. Focardi, A. C. Gossard, D. H. Wu, and M. S. Sherwin, "Room temperature terahertz detection based on bulk plasmons in antenna-coupled GaAs field effect transistors", Appl. Phys. Lett. 92, 253508 (2008).

[33] A. Yu, Z. Yang, M. Cai, H. Zhang, Z. Tian, X. Guo, L. Wang, A. V. Balakin, A. P. Shkurinov,

and Y.M. Zhu, "Graphene plasmons-enhanced terahertz response assisted by metallic gratings", Nanophotonics 11, 4737-4745 (2022).

[34] A. Yu, "Polarization-independent enhancement of graphene plasmons by coupling with the dipole-like near field of the metallic split-mesh structure", RSC Adv. **8**, 22286 (2018).

[35] X. Zang, B. Yao, L. Chen, J. Xie, X. Guo, A. V. Balakin, A. P. Shkurinov, and S. Zhuang, "Metasurfaces for manipulating terahertz waves", Light-Adv. Manuf. **2**, 10 (2021).

[36] J. Wang, D. Chen, Z. Wang, Q. Xue, and X. Sun, "Focusing enhanced broadband metalens via height optimization", Opt. Lett. **18**, 72-76 (2022).

Declaration of Interest Statement

The authors declare that they have no known competing financial interests or personal relationships that could have appeared to influence the work reported in this paper.